Synthesis and Characterization of Porous Vanadium Silicates in Organic Medium

Vittorio Luca,*,† Dugald J. MacLachlan,† and Keith Morgan‡

Research School of Chemistry, The Australian National University, Canberra, ACT 0200, Australia, and Industrial Research New Zealand Limited, Gracefield Road, P.O. Box 31-310, Lower Hutt, New Zealand

Received December 6, 1996. Revised Manuscript Received June 18, 1997⊗

Porous vanadium silicates have been synthesized in ethanolic medium by base hydrolysis of a mixture of tetraethoxysilicon(IV) and cetyltrimethylammonium vanadate precursors. The materials are similar to mesoporous silicates such as MCM-41 but have smaller pores and specific surface areas ranging from 270 to 1100 m^2/g for samples with vanadium concentrations from 32 to 8 at. %. Using a variety of techniques, it is shown that the synthesis method results in isolated tetrahedral vanadate units homogeneously incorporated into and on the silicate matrix. On calcination, a similar vanadium coordination is found, but adsorption of water causes cleavage of Si−O−V bonds to give a mixture of isolated tetrahedral vanadium species in addition to polymeric vanadates and vanadium oxides. Nevertheless, the vanadium in these samples appears to be in a highly dispersed state. Silicon-29 MAS NMR of uncalcined samples shows that the degree of SiO_4 condensation decreases with increasing vanadium content. The thermal stability appears to depend on establishing a well-condensed pore wall that occurs for samples containing up to 11 at. % vanadium. For samples containing vanadium concentrations greater than about 15 at. % the pore structure is unstable and ruptures on exposure to moist air. The vanadium silicates are compared to vanadia−silica aerogels and MCM-41.

Introduction

The homogeneous dispersion of metallic elements on the surfaces and/or within the structure of high surface area inert and semiconducting oxide supports such as SiO_2 and TiO_2 has been the goal of the catalyst researcher for many years. A similar goal has been pursued by the molecular sieve scientist in incorporating transition metal ions in the framework of zeolite and phosphate molecular sieves. Substitutions of this kind have yielded materials with extremely interesting catalytic properties. Often, the degree of substitution of the heteroatom into the molecular sieve framework is extremely limited, and there are relatively few examples of true end-member non-silicon microporous oxides.

Recently, the micelle-forming ability of surfactant molecules has been exploited in the synthesis of a family of amorphous silicates known as M41S that have extremely large and uniform pores.[1−4] It was shown that the pore size of these mesoporous silicates could be tuned in the range 20−100 Å by suitable selection of surfactant chain length as well as the co-addition of organic spacer molecules. Detailed characterization of the structure of these new silicates as well as a possible mechanism for their formation involving the templating action of the surfactant micelles has since followed.[5] Because of its importance in selective catalytic reduction and oxidation reactions, there have been numerous attempts to incorporate vanadium into the framework of zeolites and M41S materials. In the latter case, only relatively low amounts of V have so far been incorporated by addition of a vanadium salt to the reaction mixture at some point during synthesis. For example, Reddy et al.[6,7] have reported MCM-41 products with 1.6 at. % V, while Zhang and Pinnavaia[8] have reported MCM-48 containing 1.9 at. % V.

It is well-known that the size and shape of surfactant micelles are dependent on factors such as electrolyte concentration and solvent.[9] This suggests that it may be possible to effect additional control over pore size and shape by performing syntheses in media other than water. In this vein, we recently reported the synthesis of a mesostructured vanadium oxide phase from alcoholic solution at room temperature using the cetyltrimethylammonium (CTA) vanadate salt precursor rather than the chloride or bromide salts that are most often employed in the synthesis of M41S materials.[10] The dissolution of this precursor in ethanol results in a

* To whom correspondence should be addressed. Present address: School of Chemistry, University of New South Wales, Sydney 2052, Australia.
† Australian National University.
‡ Industrial Research New Zealand Limited.
⊗ Abstract published in *Advance ACS Abstracts,* October 15, 1997.

(1) Kresge, C. T.; Leonowicz, M. E.; Roth, W. J.; Vartuli, J. C.; Beck, J. S. *Nature* **1992**, *359*, 710.
(2) Beck, J. S.; Chu, C. T.-W.; Johnson, I. D.; Kresge, C. T.; Leonowicz, M. E.; Roth, W. J.; Vartuli, J. C. U.S. Patent 1992 5 108 725.
(3) Beck, J. S.; Leonowicz, M. E.; Roth, W. J.; Vartuli, J. C. U.S. Patent 1992 5 102 643.
(4) Beck, J. S.; Vartuli, J. C.; Roth, W. J.; Leonowicz, M. E.; Kresge, C. T.; Schmitt, K. D.; Chu, C. T.-W.; Olson, D. H.; Sheppard, E. W.; McCullen, S. B.; Higgins, J. B.; Schlenker, J. L. *J. Am. Chem. Soc.* **1992**, *114*, 4, 10834.
(5) Monnier, A.; Schuth, F.; Huo, Q.; Kumar, D.; Margolese, D. I.; Maxwell, R. S.; Stucky, G. D.; Krishnamurty, M.; Petroff, P. M.; Firouzi, A.; Janicke, M.; Chmelka, B. F. *Science* **1994**, *261*, 1299.
(6) Reddy, K. M.; Moudrakovski, I.; Sayari, A. *J. Chem. Soc., Chem. Commun.* **1994**, 1059.
(7) Reddy, J. M.; Sayari, A. *J. Chem. Soc., Chem. Commun.* **1995**, 2231.
(8) Zhang W.; Pinnavaia, T. J. *Catal. Lett.* **1996**, *38*, 261.
(9) Mittal, K. L.; Lindman, B. *Surfactants in Solution*; Plenum Press: New York, 1984.

S0897-4756(96)00621-7 CCC: $14.00

Table 1. Chemical Analyses and Thermal Data for Vanadosilicate Samples

sample	atom % V added	atom % V in products	% wt loss[a]	S_{BET} (m^2/g)
VS−8	9	8	31	1120
VS−11	11	11	34	850
VS−13	17	13	37	690
VS−14	20	14	43	435
VS−15	25	15	44	270
VS−20	33	20	45	
VS−32	50	32	54	

[a] Second weight loss occurring between 25 and 250 °C.

single discrete vanadate species, making it possible to effect a "clean" and controlled condensation of the vanadate by slow addition of dilute HCl. Furthermore, by eliminating as much competition as possible between various anionic solution species for the micelle interface the hydrolysis/condensation reactions are presumed to occur at or close to the charged micelle surface. The mesostructured vanadium oxide showed thermal stability to about 200 °C, at which point only incomplete removal of the surfactant had been achieved.

In an attempt to improve thermal stability of vanadium-containing mesoporous materials and further explore syntheses in nonaqueous media, we now focus on the synthesis of surfactant-derived porous vanadium silicate materials again using CTA-vanadate as a precursor. It was also hoped that, by using this more controlled approach, materials of higher stability and having a high degree of vanadium dispersion might eventuate. Characterization of these binary oxide systems was carried out using powder X-ray Diffraction (XRD), ^{51}V and ^{29}Si solid-state nuclear magnetic resonance (NMR), electron paramagnetic resonance (EPR)/electron spin−echo modulation (ESEM), FTIR/Raman, and UV−vis spectroscopies.

Experimental Section

The porous vanadium silicates were synthesized from an alcoholic solution containing the cetyltrimethylammonium vanadate salt (CTAV). The vanadate salt was isolated as previously described.[10] In a typical synthesis, 1.07 g of the CTA-vanadate was dissolved in 80 mL of ethanol to which was added tetraethoxy silane (TEOS) to give a calculated mole ratio of vanadium to silicon. To this was added 10 mL of water and the pH adjusted to 10.0 with a few drops of tetramethylammonium hydroxide (TMAOH). At this stage, the solution was colorless, but after refluxing for about 30 min a white product formed. Refluxing was continued for a further 3 h, after which time the product was filtered, thoroughly washed with ethanol, and dried in ambient air. Other samples were made by holding the CTA-vanadate concentration and solution volume constant and adding varying amounts of TEOS. The amount of water added was more than required to effect stoichiometric hydrolysis of the TEOS.

Energy-dispersive X-ray (EDX) analyses were carried out using a Tracor Northern EDX analysis system attached to a Cambridge S360 scanning electron microscope. Analysis of all the products (Table 1) indicates that the atomic percentage, $R = V/(Si + V) \times 100$, of the products was lowered relative to that of the synthesis mixture, although appreciable amounts of vanadium were retained. From here on products will be denoted as VS-R.

Electron spin−echo modulation (ESEM) data were recorded on a home-built spectrometer operating at 9−10 GHz. Two-pulse echoes were obtained using a $\pi/2 - \tau - \pi$ pulse sequence. Three-pulse stimulated echo data were recorded using a phase cycled $\pi/2 - \tau - \pi/2 - T - \pi/2$ pulse sequence and the echo was detected as a function of T.

Vanadium-51 NMR spectra were acquired using two different spectrometers. A Bruker MSL 300 spectrometer operating at 78.9 MHz was used to acquire ^{51}V spectra of the dehydrated samples. A $\pi/12$-acquire pulse sequence was used with a 1 s recycle delay. The preacquisition delay used was 6 μs. A Varian Unity 500 spectrometer was used to acquire spectra of uncalcined samples. Samples were packed into 5 mm rotors and spun at speeds of 12 kHz in a super-sonic, single-tuned probe from Doty Scientific. Spectra were recorded using a single-pulse experiment using pulse repetition times of 1 s. Chemical shifts are referenced to $VOCl_3$ with ammonium vanadate being used as a secondary reference.

Silicon-29 spectra were recorded on a Bruker MSL 300 spectrometer operating at 59.61 MHz using a $\pi/6$ pulse and a recycle delay of 10 s. Chemical shifts are given with respect to tetramethylsilane using kaolinite as a secondary reference.

X-ray diffraction patterns were recorded on a Siemens D5000 X-ray powder diffractometer using Cu Kα radiation.

FTIR spectra were recorded on a Perkin-Elmer spectrometer with samples pressed in KBr disks.

Raman spectra were recorded on a Renishaw Raman microscope using an argon ion laser ($\lambda = 514.5$ nm). Spectra were recorded at the lowest possible laser power level consistent with reasonable signal-to-noise ratio in order to avoid effecting changes to the nature of the surface species due to sample heating by the laser beam.

Nitrogen adsorption isotherms were measured using a Sartorius microbalance at 77 K. Pressure was monitored with a Hastings model 760 gauge interfaced to a PC. Samples were pretreated at 350 °C in air for 24 h prior to measurement, and no special precautions were taken to exclude the adsorption of atmospheric moisture. Where applicable, pore size distributions were determined by the Barrett−Joyner−Halenda (BJH) method in which a cumulative pore volume in the maximum range 1.7−300 nm is assumed.

Results

SEM/XRD. The present synthesis procedure produces smooth flat particles of 1−2 μm diameter as exemplified in the SEM image of the VS-15 sample after calcination at 350 °C (Figure 1). This particle morphology is retained up to 32 at. %.

Figure 2 shows XRD traces in the 0.8−10° 2θ range of products having various concentrations of vanadium. XRD patterns of products with less than 25 at. % V (Figure 2a−d) consisted of a single broad reflection at low 2θ. The d-spacings for these products generally decreased from 34 to 27 Å as the vanadium content increased. For VS-32 (Figure 2e) the d-spacing of the major peak was significantly smaller and the peak width narrower than products with lower V concentration. Also, a higher angle peak was present that appears to be a higher order of the main reflection. The XRD trace of the CTA-vanadate salt (Figure 2f) has a main reflection at 27 Å, and higher order reflections out to at least the seventh order can be discerned. A smaller peak flanking the main reflection at 27 Å is possibly due to a separate layered phase involving higher vanadium polymers.

Calcination of samples was carried out in air at 350 °C followed by rehydration in ambient air and XRD patterns of selected samples are shown in Figure 3. The XRD patterns of VS-8 and VS-11 shown in Figure 3a,b indicate that these samples are relatively stable after this calcination treatment. The XRD patterns of VS-8 and VS-11 samples calcined at 500 °C and allowed to rehydrate in ambient air were little different to those

(10) Luca, V.; MacLachlan, D. J.; Hook, J. M.; Withers, R. *Chem. Mater.* **1995**, 7, 2220.

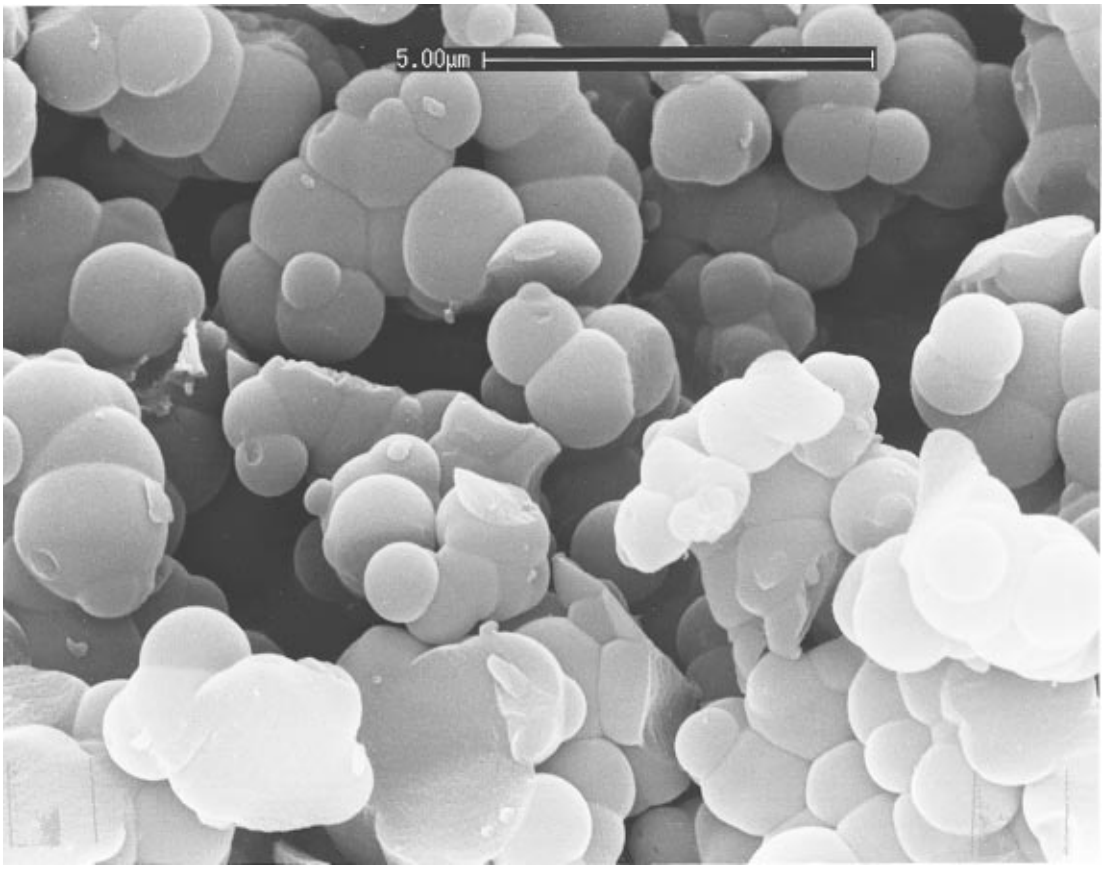

Figure 1. SEM photograph showing morphology of uncalined VS-11 particles.

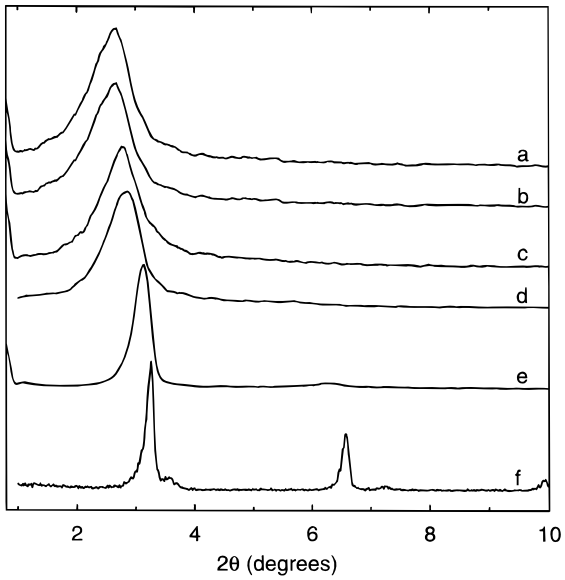

Figure 2. Powder XRD patterns of uncalcined (a) VS-8, (b) VS-11, (c) VS-13, (d) VS-15, (e) VS-32, and (f) CTA-vanadate.

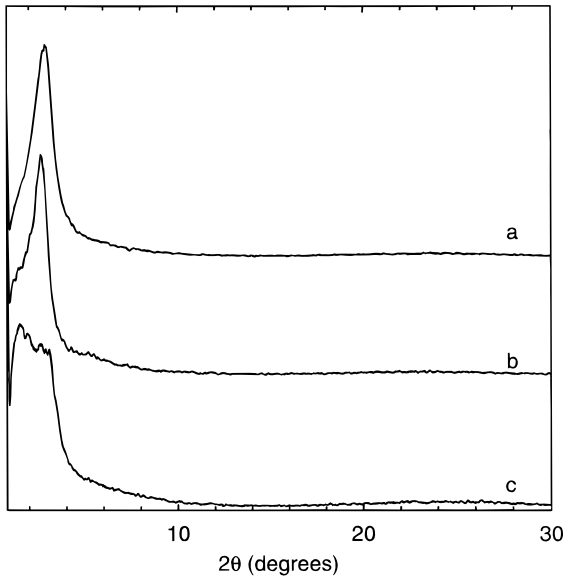

Figure 3. Powder XRD patterns of calcined and rehydrated (a) VS-8, (b) VS-11, and (c) VS-15.

of samples calcined at 350 °C. The X-ray pattern beyond 10°2θ contained no further peaks at both calcination temperatures showing that crystalline vanadium oxides are not formed.

Calcination of samples with greater than 13 at. % V at 350 °C causes broadening and splitting of the low-angle reflection, but again no crystalline phases are observed by XRD. For the VS-15 sample (Figure 3c), the broad low-angle reflection is composed of two components, one at about 54 Å and the other at about 32 Å. Similar results were obtained with the samples containing from 14 to 20 at. % vanadium. For VS-32 calcined at 350 °C, no XRD peaks were observed in the low-angle region, but at higher angles weak and broad peaks from vanadium pentoxide could be discerned. This is to be contrasted with recently synthesized vanadia–silica aerogels made by the solution–sol–gel route that begin to show peaks from vanadium oxides at the 22 at. % loading prior to heating.[11] This suggests that an excellent dispersion of vanadium has been achieved in the present materials.

(11) Dutoit, D. C. M.; Schneider, M.; Fabrizioli, P.; Baiker, A. *Chem. Mater.* **1996**, *8*, 734.

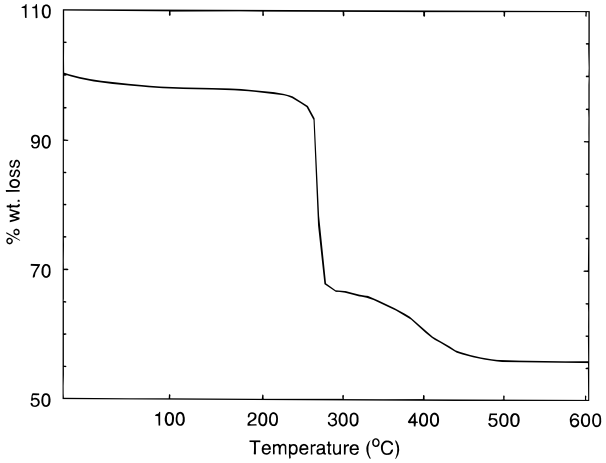

Figure 4. TGA trace of VS-15 in air and using a heating rate of 10 °C/min.

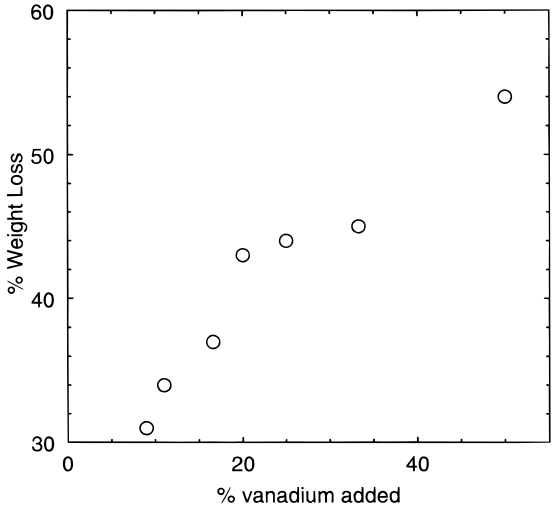

Figure 5. Percentage weight loss in the 250−300 °C temperature range for vanadium silicates synthesized from reactant solutions containing different initial V concentrations.

It is important to emphasize that, apart from the concentrated VS-32 sample, no crystalline phases were detected in the XRD pattern of any of the other samples even when the calcination temperature was as high as 500 °C.

Thermogravimetric Analysis (TGA). TGA traces of all the vanadium silicates shared similar characteristics, and only the data for VS-15 are shown in Figure 4. Two regions of weight loss could be identified, and these are listed for the various samples in Table 1. A minor progressive weight loss of about 8 wt % occurs between 25 and 260 °C followed by a steep loss at about 300 °C. The abrupt kink that occurs during this second weight loss is due to the combustion of the organic as the TGA traces were recorded in flowing air. It appears therefore that calcination in air at temperatures as low as 300 °C suffices to remove the surfactant. This is confirmed by FTIR spectra, which show neither C−C nor C−H stretching frequencies after calcination at temperatures around 300−350 °C. Therefore, in this study, samples were generally not heated much in excess of that necessary to completely remove the surfactant. The magnitude of the second weight loss is plotted in Figure 5 against the amount of vanadium added as CTA-vanadate during the synthesis. This shows that there is no limiting value to the amount of surfactant incorporated.

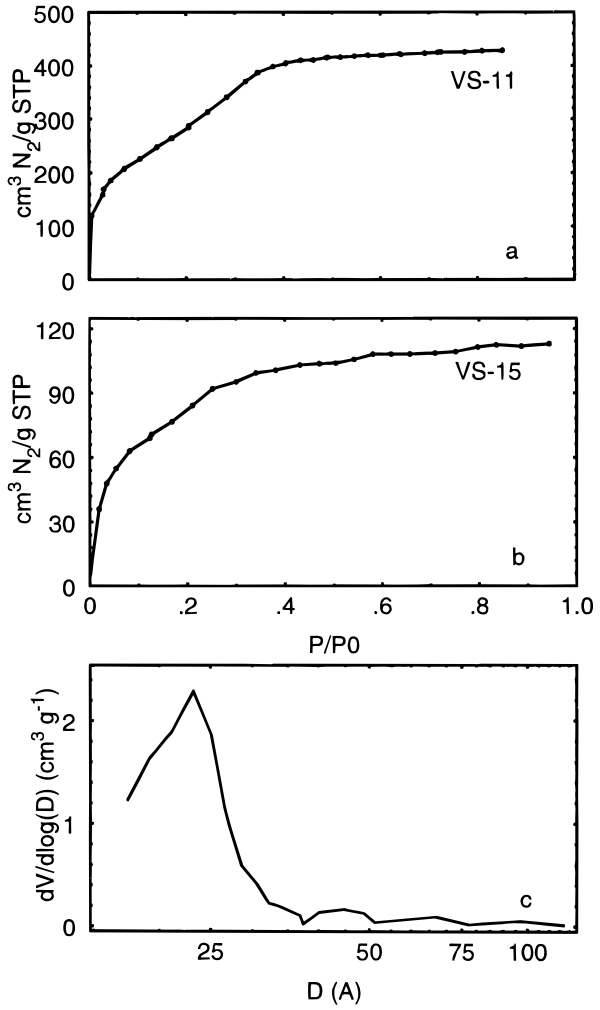

Figure 6. N_2 adsorption isotherms at 77 K of (a) VS-11and (b) VS-15 calcined at 350 °C, and (c) BJH pore size distribution for sample from (a).

N_2 Adsorption. Nitrogen adsorption isotherms of a selection of the vanadium silicates synthesized in the present study are shown in Figure 6. Calculated surface areas were 270, 850, and 1120 m^2/g for samples containing 15, 11, and 8 at. % V, respectively (Table 1). The shape of the isotherms for samples containing from 8 to 14 at. % V match most closely those of the type IV classification, indicating mesoporosity. However, the inflection becomes less pronounced as the V concentration increases and is not visible at all for V concentrations greater than ca. 15 at. %, suggesting absence of mesoporosity. For samples with isotherms displaying a shallow step, this step occurs at P/P0 ∼ 0.2 rather than P/P0 ∼ 0.4 as observed for MCM-41 materials.[12] An example of a pore size distribution obtained from the VS-11 sample is shown in Figure 6c. This pore size distribution is very broad and is centered at about 23 Å, confirming that the pores are significantly smaller than for MCM-41 materials synthesized using the same surfactant with average pore sizes of 38 Å. The relatively high surface areas obtained together with isotherm shapes and large particle sizes observed by

(12) Branton, P. J.; Hall, P. G.; Sing, K. S. W.; Reichert, H.; Schüth, F.; Unger, K. K. *J. Chem. Soc., Faraday Trans.* **1994**, *90*, 2965.

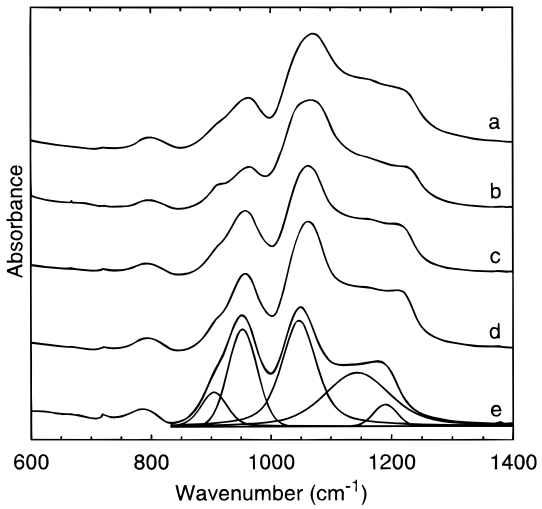

Figure 7. FTIR spectra of uncalcined (a) VS-8, (b) VS-11, (c) VS-13, (d) VS-15, and (e) VS-32, together with spectral decomposition.

SEM suggest that the present samples undergo a transition from mesoporous to microporous as the proportion of vanadium increases.

Vibrational Spectroscopy. FTIR spectra of the uncalcined samples are shown in Figure 7. The bands around 1050−1230 cm^{-1} are due to silicate anions, while a number of bands are also evident at 960 and 920 cm^{-1}. Bands in this frequency range in spectra of zeolites substituted with Ti and V have been thoroughly studied and apparently involve Si−O stretching of $[O_3Si-O]^{\delta-}$ units surrounding Ti and V atoms.[13] Therefore, the presence of a band at 960 cm^{-1} has generally been adopted as evidence for the substitution of heteroatoms such as Ti, V, and Fe into zeolite frameworks.[14] It has recently also become customary in the study of porous V- and Ti-containing silica gels to attribute bands around 960 cm^{-1} to V−O−Si bonds or Ti−O−Si.[15]

The spectra in the region 850−1400 cm^{-1} have been decomposed into their components, and an example decomposition is shown in Figure 7e. Spectra of calcined and uncalcined samples required five components to achieve a satisfactory fit. Bands at around 910 and 960 cm^{-1} are assigned to ν(V−O−Si) stretching vibrations as discussed above, while the band around 1060 cm^{-1} can be assigned to ν(Si−OH) and those at 1140, and 1220 cm^{-1} to asymmetric ν(Si−O−Si) stretching modes as outlined previously.[11,15] For a measure of Si−O−V connectivity we define the parameter S, which is the ratio of the intensity of the bands at 910 and 960 cm^{-1} to the total intensity in the 900−1400 cm^{-1} region. The results are listed in Table 2 for both the calcined and uncalcined samples. The value of the parameter S follows roughly the increase in V concentration, showing that most of the added vanadium forms Si−O−V units.

FTIR spectra after calcination are shown in Figure 8 and indicate a large reduction in the Si−O−V concentration relative to that of the uncalcined counterparts.

Table 2. Percentage of Various Si Sites Found by Spectral Decomposition of ^{29}Si MAS-NMR and Value of Parameter *S* Obtained from Decomposition of FTIR Data in the Range 800−1400 cm^{-1} for Selected Vanadium Silicate Samples

sample	%Q^2	%Q^3	%Q^4	S^a
VS−8	3.6	33.1	63.2	16.4
VS−11	5.0	36.9	58.2	12.3
VS−14	7.8	30.2	62.0	22.3
VS−15	6.2	56.6	37.3	21.7
VS−20	4.8	48.0	47.2	
VS−32	9.2	90.8	0	30.1
$VS-8_{350}$				8.8
$VS-11_{350}$				6.5
$VS-13_{350}$				12.0
$VS-15_{350}$				10.2

[a] Decomposition of FTIR spectra $S = I_{960} + I_{920}/I_{tot}$.

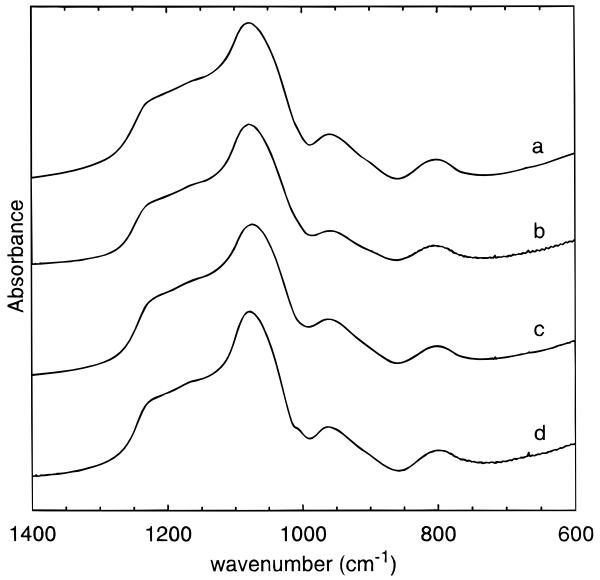

Figure 8. FTIR spectra of V-silicates calcined at 350 °C in air and rehydrated: (a) VS-8, (b) VS-11, (c) VS-13, (d) VS-15.

The fact that there is less of a difference in the Si−O−V concentrations between the samples after calcination hints at some limiting value for the amount of V that can be incorporated in the pore walls and still yield a stable structure.

Raman spectra of the precursor CTA-vanadate salt together with the VS-15 sample before and after calcination (Figure 9) are representative of all of the samples studied. The broad band at 921 cm^{-1} and the sharp intense band at 943 cm^{-1} in the Raman spectrum of the CTA-vanadate precursor can be assigned to vibrations of the vanadate anion by comparison with the spectrum of the CTA-bromide (not shown). These bands together with many of the other bands observed in the spectrum of the CTA-vanadate salt are also observed in the VS-15 product although they are somewhat broader. This indicates that the vanadate units remain intact in the products experiencing little change in symmetry. Calcination results in removal of these bands and the appearance of a broad band at 1030 cm^{-1} (Figure 9c). Such a band is consistent with that normally observed for SiO_2-supported vanadate species $O{=}V{-}O_3{-}SiO_2$ that are either isolated or in chains that vibrate at 1042 cm^{-1} [16,17] rather than crystalline V_2O_5-type phases that possess an intense band at around 993 cm^{-1}.[18,19] This is an important result since it demonstrates that even

(13) Scarano, D.; Zecchina, A.; Bordiga, S.; Geobaldo, F.; Spoto, G.; Petrini, G.; Leofanti, G.; Padovan, M.; Tozzola, G. *J. Chem. Soc., Faraday Trans.* **1993**, *89*, 4123.

(14) Kornatowski, J.; Sychev, M.; Kuzenkov, S.; Strnadova, K.; Pilz, W.; Kassner, D.; Pieper, G.; Baur, W. H . *J. Chem. Soc., Faraday Trans.* **1995**, *91*, 2217.

(15) Dutoit, D. C. M.; Schneider, M.; Baiker, A. *J. Catal.* **1995**, *153*, 165.

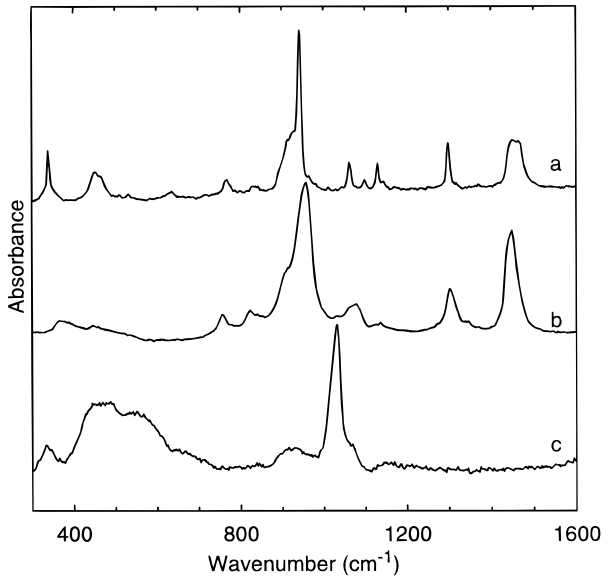

Figure 9. Raman spectra of (a) CTA-vanadate precursor, (b) uncalcined VS-15, (c) VS-15 calcined at 350 °C and rehydrated.

after water adsorption a significant proportion of the vanadium remains in a highly dispersed state.

^{51}V NMR. In principle, both static and MAS ^{51}V NMR can give information on the chemical environment of vanadium through the chemical-shielding anisotropy, which depends on factors such as coordination number, degree of condensation, and site symmetry.[20] This technique has therefore been extensively deployed in the characterization of supported vanadium oxide catalysts.[20,21] If the nuclear Zeeman interaction is significantly greater than the quadrupolar perturbation, the central transition line shape remains unaffected by the quadrupolar interaction to first order. In this case, the principal chemical-shielding components can be determined directly from the static spectrum provided that the separation of the powder turning points are greater than the experimental line width. In cases where the electric quadrupole perturbation extends to second order, the central transition line shape will be affected and a simple line shape may not be observed. Because the second-order quadrupole perturbation and the chemical-shielding anisotropy have the opposite dependence on magnetic field measurements at more than one field are sometimes necessary.

Similar static ^{51}V NMR spectra were obtained for all of the uncalcined samples regardless of V concentration. Representative spectra for VS-15 and VS-32 are shown in Figure 10a,b. These static powder patterns are indicative of rhombic symmetry with three turning points being observed at about −440, −540, and −840 ppm. This gives an anisotropy, $\Delta\delta = \delta_{33} - \delta_{11}$, of about 400 ppm. The base-line roll in these spectra is due to slight distortions of the FID introduced by dead-time,

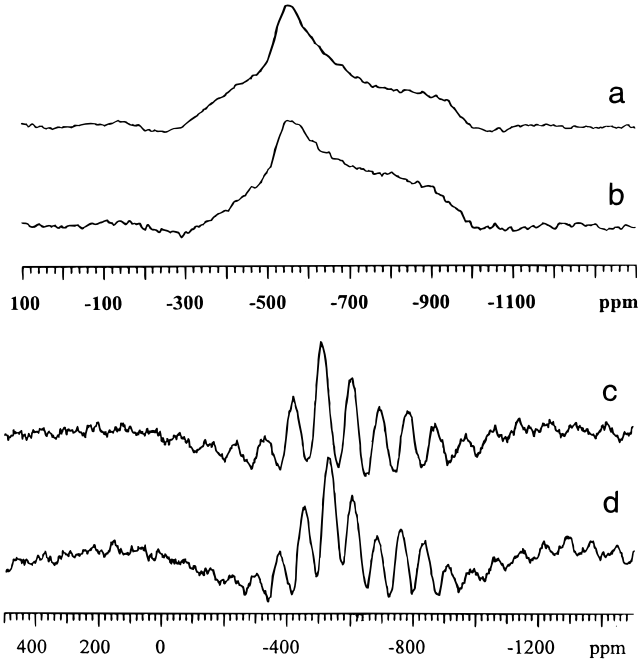

Figure 10. Static ^{51}V NMR spectra at 500 MHz of uncalcined (a) VS-13, (b) VS-32 and 12 kHz ^{51}V MAS NMR spectra of uncalcined (c) VS-13, (d) VS-32.

which is caused by the resonator ring down. For spectra recorded at 500 MHz, this base-line role was not removed. Although no attempt was made to determine precise values for the principal shift components, the approximate values extracted by inspection of the spectra gave anisotropies of about 400 ppm. This value limits the connectivity to at most Q^2.[20] The value of n in the Q^n notation denotes the number of vanadium atoms linked via oxygen bridges to a central vanadium atom. There was no indication in the static spectra of any of the uncalcined samples of an octahedral species that would exhibit an axial tensor with $\delta_\perp = -300$ ppm and $\delta_{||} = -1250$ ppm. MAS NMR spectra of the uncalcined VS-15 and VS-32 samples are shown in Figure 10c,d. Irrespective of V concentration, only a single resonance was observed under MAS conditions with $\delta_{iso} \approx -605$ ppm. Note that the δ_{iso} values are uncorrected for possible quadrupolar shift, although this would seem to be small on the basis of the general observation that the chemical shift values recorded at 300 and 500 MHz were the same.

Static NMR spectra of samples that had been calcined and prevented from absorbing atmospheric moisture are shown in Figure 11. The static spectrum of VS-13 (Figure 11a) that was similar to that obtained for samples with lower V concentrations is dominated by a single symmetrical peak at −460 ppm but also contains a minor feature at about −1050 ppm. There is no intensity around −300 ppm in this spectrum where $\delta_\perp$ of V_2O_5-like phases would occur. Only a single species was observed in the MAS spectrum of these samples with $\delta_{iso} = -709$ ppm.

Das et al.[22] have studied model compounds in which V is in distorted tetrahedral coordination and found near axial shielding tensors ($\delta_1 = -510$, $\delta_2 = -525$, $\delta_3 = -1150$). This tensor is similar to that obtained for

(16) Schrami-Marth, M.; Wokaun, A.; Pohl, M.; Krauss, H.-L. *J. Chem. Soc., Faraday Trans.* **1991**, *87*, 2635.
(17) Went, G. T.; Oyama, S. T.; Bell, A. T. *J. Phys. Chem.* **1990**, *94*, 4, 4240.
(18) Sanchez, C.; Livage, J.; Lucazeau, G. *J. Raman Spectrosc.* **1982**, *12*, 68.
(19) Claws, P.; Broeckx, J.; Vennik, J. *Phys. Stat. Solidi* **1985**, *131*, 459.
(20) Eckert, H.; Wachs, I. E. *J. Phys. Chem.* **1989**, *93*, 6796.
(21) Lapina, O. B.; Mastikhin, V. M.; Shubin, A. A.; Krasilnikov, V. N.; Zamaraev, K. I. *Prog. NMR Spectrosc.* **1992**, *24*, 457.
(22) Das, N.; Eckert, H.; Hu, H.; Wachs, I. E.; Walzer, J. F.; Feher, F. J. *J. Phys. Chem.* **1993**, *97*, 8240.

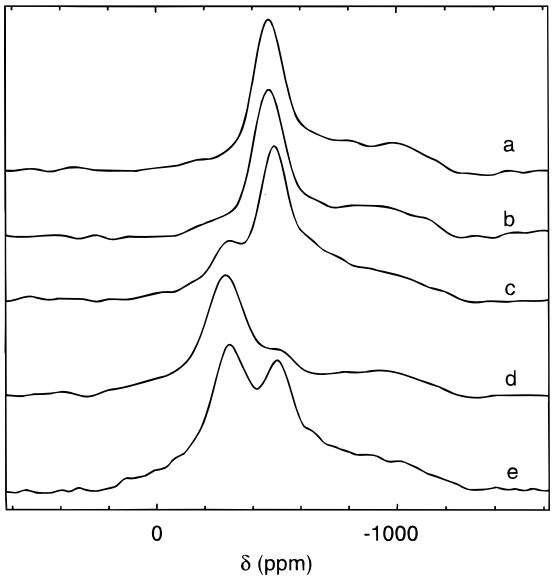

Figure 11. Static ^{51}V NMR spectra (MHz) of calcined and dehydrated (a) VS-13, (b) VS-15, (c) VS-32, and calcined and rehydrated (d) VS-13, and (e) VS-32.

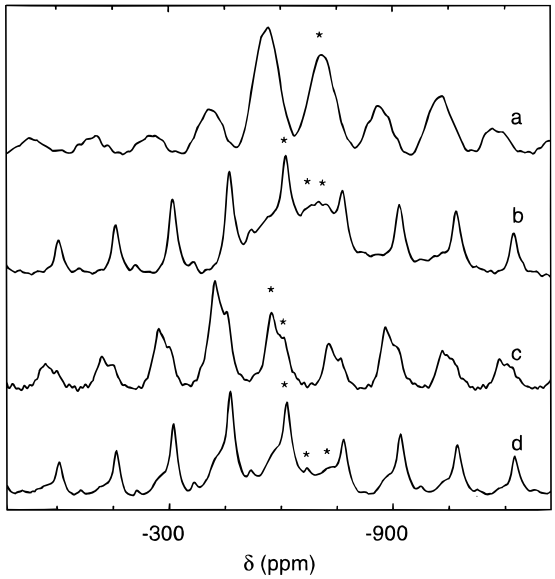

Figure 12. ^{51}V MAS (12 kHz) NMR spectra of uncalcined and dehydrated (a) VS-13 and (b) VS-32 and calcined and rehydrated (c) VS-13 and (d) VS-32. Isotropic peaks that are uncorrected for possible second-order quadrupolar perturbation are indicated by an asterisk.

all of the present dehydrated samples. Thus, there has been quite a dramatic change in the chemical environment after removal of the template, although it seems that a distorted tetrahedral symmetry is being preserved. Similar ^{51}V NMR spectra have recently been described by Morey et al.[23] for V dispersed on the surfaces of dehydrated MCM-48 and assigned as tetrahedral vanadium. The most concentrated samples studied by this group had 10.7 at. % V on the MCM-48 surface. On this basis, therefore, the most likely assignment for the static spectra of the uncalcined samples with low V concentrations is to an axial, or near axial, shielding tensor ($\delta_\perp = -460$ and $\delta_{||} = -1100$ ppm) of a single tetrahedral V species in which the anisotropy is considerably reduced compared to bulk V_2O_5 ($\delta_\perp = -280$; $\delta_{||} = -1250$ ppm; $\delta_{iso} = -609$ ppm).

As the V concentration is increased an additional feature at about −280 ppm is suggestive of octahedral coordination is observed in the static spectrum of dehydrated VS-15 (Figure 11c). This resonance attained significant intensity in the static spectrum of VS-32. Although the resonance at −280 ppm indicates an octahedral coordination, the negligible intensity of any additional powder features precludes a definitive assignment to V_2O_5-like phases on the basis of the static spectrum alone. However, support for the assignment of the −280 ppm resonance in the static spectra to clusters of VO_6 polyhedra resembling those in V_2O_5 is provided by the MAS spectrum of the VS-32 sample (Figure 12b), which shows isotropic shifts at −614, −673, and −717 ppm. The resonance at −614 ppm coincides with that observed for bulk V_2O_5, while the resonance at −717 ppm corresponds to the species observed in the spectrum of the VS-13 and VS-15 after calcination and prior to water absorption. The attribution of the −673 ppm resonance in this spectrum is uncertain but may correspond to the polymerized vanadates observed by Raman spectroscopy. The static spectrum of the VS-32 sample (Figure 11b) is similar to the spectrum obtain by Gontier and Tuel[24] for an MCM-41 sample containing 3 mol % vanadium. However, these investigators did not record their spectra beyond −800 ppm and reported no MAS spectra.

When the dehydrated samples were allowed to rehydrate in ambient air the intensity of the −280 ppm resonance in the static spectra increased (Figure 11d,e), suggesting that further polymerization and condensation of previously isolated tetrahedral vanadate occurs. Although the static spectra of the rehydrated samples indicate that V is present in both tetrahedral and octahedral coordination, the MAS spectra (Figure 12) indicate that the situation is far more complex with the presence of three or more isotropic shifts. This can be deduced by comparison of spectra recorded at several spinning speeds and by spectral decompositions of the central region. To understand further the changes occurring on exposure to air would require a more comprehensive investigation of samples allowed to absorb known amounts of water, which is beyond the scope of the present investigation. It is noted that although significant conversion of tetrahedral to octahedral vanadium occurs on exposure to ambient air, not all of the initially tetrahedral species are converted. The NMR results are in agreement with the FTIR data and suggest that some vanadium remains incorporated in the pore walls.

A portion of the VS-13 sample that had been briefly exposed to air was stirred overnight in water and then filtered and washed with further water. This sample gave no ^{51}V NMR spectrum indicating that most of the diamagnetic vanadium had been removed by this treatment. In contrast, samples with comparable V loadings that were exposed to ambient air for periods of weeks could be washed with water without losing their deep orange coloration. It is clear that the nature of the V phase ultimately formed depends on the duration of exposure to ambient air and that after longer times the

(23) Morey, M.; Davidson, A.; Eckert, H.; Stucky, G. *Chem. Mater.* **1996**, *8*, 486.

(24) Gontier, S.; Tuel, A. *Micorposous Mater.* **1995**, *5*, 161.

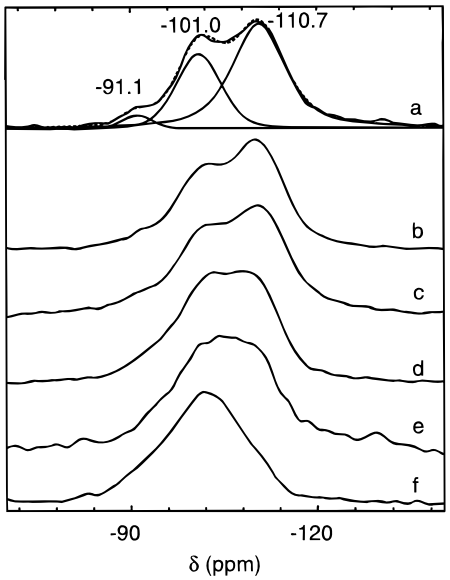

Figure 13. ^{29}Si MAS (4 kHz) NMR spectra of uncalcined (a) VS-8, (b) VS-11, (c) VS-13, (d) VS-15, (e) VS-20, and (f) VS-32. Numbers above peaks in (a) are the chemical shifts in ppm relative to TMS.

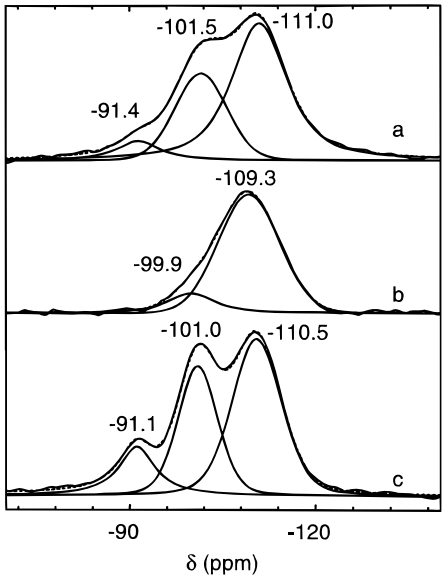

Figure 14. ^{29}Si MAS (4 kHz) NMR spectra of (a) uncalcined VS-14, (b) dehydrated sample from (a) calcined at 350 °C in air for 24 h, and (c) sample from (b) exposed to air. Numbers above peaks are chemical shifts in ppm relative to TMS.

degree of aggregation is greater and the removal of these larger clusters by washing becomes more difficult.

^{29}Si MAS NMR. Silicon-29 MAS NMR spectra of the various uncalcined samples are shown in Figure 13. These spectra were decomposed into the minimum number of peaks required to give an acceptable fit, and the fit results are given in Table 2. Between two and three peaks were usually required for satisfactory fits, and these had shifts at −90, −100, and −111 ppm that are usually associated with Q^2, Q^3 and Q^4 silicons. There is a clear trend toward increasing relative intensity of the resonance at −100 ppm with increasing vanadium concentration. The spectra and spectral decompositions obtained for samples with low V concentration are similar to those reported for all-silica MCM-41 materials.[25]

Figure 14 shows the effect of calcination at 350 °C in air on VS-14, which has intermediate V concentration. The spectrum of this sample was recorded after heating without allowing the adsorption of water by loading the NMR rotor under dry nitrogen. This sample remained white before and after acquisition of the spectrum, indicating that no significant water had been adsorbed. Silicon-29 MAS NMR spectra recorded before (Figure 14a) and after (Figure 14b) calcination without water adsorption are quite different, with the latter being dominated by a resonance at −109 ppm. When this sample was exposed to air for about 2 h it became yellow, and its ^{29}Si NMR spectrum resembles that of the uncalcined material in terms of the different Si sites observed and their relative proportions.

EPR/ESEM. The 4 K EPR spectra of VS-13 after calcination followed by immediate evacuation and after equilibration in ambient air are shown in Figure 15. These spectra have been simulated using an axial spin Hamiltonian with similar parameters except that the parallel parameters are measurably different ($g_{||} = 1.92$, $A_{||} = 190$ G compared with $g_{||} = 1.930$, $A_{||} = 200$ G).

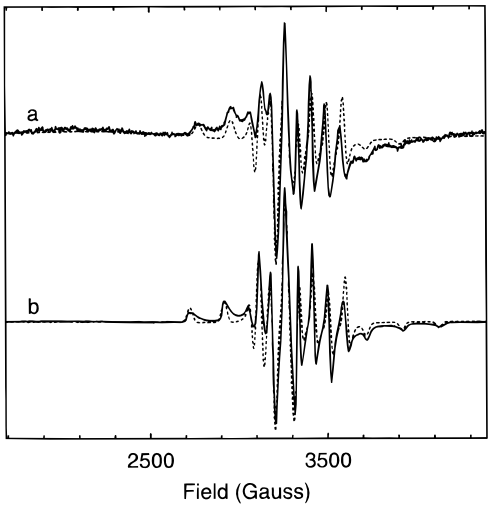

Figure 15. Experimental (solid line) and simulated (dashed line) EPR spectra of (a) uncalcined VS-14, (b) sample from (a) calcined and evacuated.

The parallel parameters for the air-equilibrated sample are quite similar to those expected for the $VO(H_2O)_5^{2+}$ ion. When the sample that had been exposed to ambient air was washed with water the 4 K EPR spectrum of Figure 15b resulted. This spectrum is identical with that of the air-equilibrated sample, and its assignment to $VO(H_2O)_5^{2+}$ that is no longer surface bound is confirmed by the fact that at 298 K an eight-line spectrum is observed that can be attributed to the rapid reorientational averaging of the **g**- and **A**-anisotropy. The spectrum recorded at 298 K, however, continues to show a dipolar broadened line indicating that some of the paramagnetic vanadium is in the form of clusters or patches in which the V−V distance is relatively small.

For a paramagnetic V center that is essentially isolated from other similar centers a well-resolved CW-EPR spectrum would be obtained, but this does not mean that the V^{4+} is isolated from V^{5+}. If the V^{4+} or VO^{2+} were diluted in a vanadia cluster containing mainly V^{5+} a well-resolved spectrum would also be

(25) Chen, C.-Y.; Burkett, S. L.; Li, H.-X.; Davis, M. E. *Microporous Mater.* **1993**, *2*, 27.

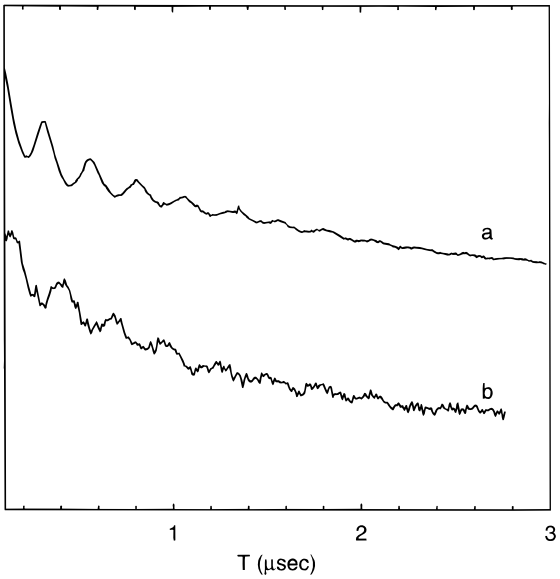

Figure 16. ESEM spectra of VS-14 (a) calcined and evacuated and (b) calcined and rehydrated.

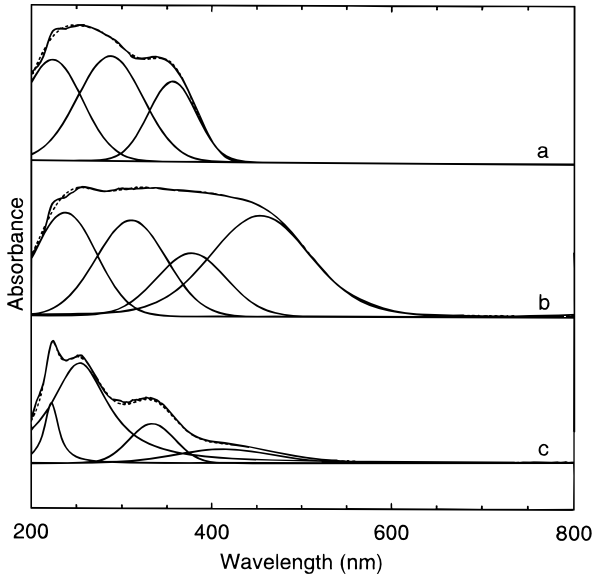

Figure 17. Experimental diffuse reflectance UV/vis spectra with spectral decompositions of VS-14 (a) uncalcined, (b) calcined and rehydrated, and (c) calcined and washed.

expected. We have previously shown that the electron spin−echo modulation (ESEM) technique is able clarify this situation since a paramagnetic V^{4+} center in the vicinity of ^{51}V would give an ESEM spectrum showing intense modulation from the nearby ^{51}V.[26] ESEM spectra of the dehydrated and rehydrated samples are shown in Figure 16. The modulation frequency observed in these data corresponds to the Larmor frequency of ^{51}V, indicating that the paramagnetic center is proximal to $^{51}V^{5+}$.

UV−vis Diffuse Reflectance. The energy of the oxygen−vanadium charge-transfer band in the UV−vis spectrum of supported vanadium oxide is strongly dependent on the coordination environment of the vanadium center. Thus, for monomeric tetrahedral vanadium two bands are observed at 238 and 290 nm, for tetrahedral vanadium in one-dimensional chains two bands at 275 and 340 nm, for vanadium in square pyramidal coordination in two-dimensional layers a single band at 412 nm, and for octahedral vanadium in multilayer lattice a single band between 460 and 480 nm (refs 16 and 23 and references therein).

UV−vis spectra of the as synthesized VS-13 sample are shown in Figure 17. The broad spectral envelope can be satisfactorily decomposed into three bands at 223, 287, and 357 nm, which is consistent with tetrahedral vanadium monomers and one-dimensional chains. In fact, the spectrum of the as-synthesized VS-13 sample prior to calcination is similar to that of the CTA-vanadate precursor (not shown), suggesting that there is almost no change in the vanadium coordination after condensation of silicate. Calcination and exposure to ambient air for several days (Figure 17b) results in the appearance of a broad absorption at lower frequencies around 450 nm in addition to the bands attributed to tetrahedral vanadate, which are within 20 nm of their values in the uncalcined sample. The band at around 450 nm clearly signals the formation of vanadium species in which vanadium is in both 5- and 6-fold coordination with oxygen. Thus, it appears that initially most of the vanadium is in tetrahedral coordination but some of this vanadium transforms to 6-fold coordination after calcination and absorption of atmospheric water. The extent of oligomerization of this octahedral vanadium is likely to be relatively limited as the development of a complete multilayer octahedral vanadium oxide lattice should give a band above about 460 nm. Similar spectra and trends were obtained for all of the samples investigated regardless of V content. Washing of the calcined sample removes most of the low-frequency band at 455 nm from 6-coordinate vanadium, leaving a weak and broad band at 416 nm (Figure 17c). This suggests that most of the partially oligomerized vanadium is easily dissolved, leaving more of the structurally bound vanadium. Note that since no NMR signal could be observed from this washed sample it is unlikely that the remaining V concentration is any greater than about 0.5% in the VS-13 sample.

Discussion

It is apparent from SEM, XRD, and the nitrogen adsorption isotherms that the materials synthesized in alcoholic medium using the CTA-vanadate precursor resemble M41S materials. Although exceedingly porous materials are formed, there appears to be poor ordering of the pores so that only a single low-angle X-ray diffraction peak is observed as well as type IV N_2-absorption isotherms for samples having less than about 15 at. % vanadium. The XRD patterns of samples containing from 8 to 13 at. % vanadium resemble those of poorly ordered MCM-41 that result when attempts are made to substitute large amounts of a heteroatom for Si. For instance, in the synthesis of Ti−HMS, an Si/Ti ratio of 85 is already sufficient to cause considerable disorder in pore distribution as evidenced by the broadening of the principal powder XRD reflection and removal of the four or five higher order reflections usually observed for the pure siliceous MCM-41.[24] The disappearance of high order reflections is also observed

(26) Luca, V.; MacLachlan, D. J. *J. Phys. Chem.*, manuscript in preparation.

for V-containing MCM-41 materials with Si/V ratios as large as 100.[27]

From ^{51}V NMR data it is clear that for the uncalcined materials the vanadium coordination is tetrahedral and that many of these tetrahedra are linked by sharing one or two oxygen atoms. This is also confirmed by both UV−vis and Raman spectroscopy with the latter showing little change in the environment of the vanadate unit between the precursor and product. FTIR results show an increase in the concentration of Si−O−V bonds that scales roughly with the V-content for these samples. These results suggest that prior to calcination vanadate species are homogeneously dispersed in the pore walls and on the pore surfaces. Almost all the V observed by NMR remains in 4-fold coordination in samples containing up to at least 15 at. % V if they are not permitted to rehydrate after calcination. For samples with considerably more V there appears to be some segregation of vanadium into a vanadium oxide phase. The data presented in this study suggest that significant quantities of vanadium in the uncalcined samples are initially homogeneously distributed in the porous silica framework and not present as an amorphous coating. If an amorphous coating were present, it is expected that calcination at temperatures as high as 500 °C would result in the crystallization of vanadium oxide as occurs for silicas impregnated with vanadium after calcination and as has been observed in the present work for the VS-32 sample.

The XRD pattern of the calcined VS-15 material consists of at least two overlapping broad peaks in the low-angle region, indicating that the thermal stability decreases with increasing vanadium content. The presence of two low-angle peaks may indicate the formation of distinct phases or possibly a significant change in the pore shape.

The ^{29}Si MAS NMR spectra of silicates and aluminosilicates are sensitive to factors such as the connectivity of SiO_4 tetrahedra as well as the presence of other cations such as Al^{3+} in neighboring cation sites.[28] In zeolites as well as other aluminosilicates a particular type of connectivity described by the value of n in $Si(OSi)_n(OX)_{4-n}$ or Q^n resonates over a range of chemical shifts that spans about 10 ppm because of variation in bonding among different silicates. These chemical shift ranges move down by about 10 ppm to more positive values for X = H with decreasing n, although there is considerable overlap between ranges. The incorporation of heteroatoms such as Al^{3+} in neighboring cation sites can also cause a shift for a Q^n chemical shift range that depends on the electronegativity of the group bonded to the oxygen of a particular silicon.[29] For the specific case of a Q^4 silicon sharing oxygen atoms with different numbers of AlO_4 tetrahedra, this results in a 5 ppm shift of the chemical shift range to more positive values for each Si−O−Al bond formed. Since V^{5+} has very similar electronegativity and ionic radius to Al^{3+}, a similar behavior might also be expected as the number of Si−O−V linkages increases. However, unless the shift arising from each Si−O−V bond equals or exceeds that for the Si−O−Al situation and because of disorder resulting in large line widths, the formation of Si−O−V bonds might not be readily observed. On the other hand, Walther et al.[30] have attributed a small shift of the Q^3 and Q^4 ^{29}Si NMR resonances by about 1.5 ppm to more positive values due to the formation of Si−O−Ti bonds in their titanium silicate gels. Since the difference in electronegativity between Si and Ti is even greater than that between Si and V the effect might be even smaller for V. The trend of increasing Q^3 concentration and line width with increasing V concentration observed for the uncalcined samples in the present study is probably due therefore to both decreased connectivity and the presence of Si−O−V.

The disappearance of Q^3 silicons following calcination without water adsorption is easily explained as due to increased condensation and is consistent with what is normally observed in silicates and mixed titanium silicate gels[31] where heating promotes condensation and therefore decreased Q^3/Q^4 ratios. Further evidence for homogeneous distribution of vanadium and the formation of considerable numbers of Si−O−V bonds comes from the fact that the Q^4 resonance in this calcined and dehydrated sample experiences a 1.7 ppm shift to more positive values relative to the uncalcined sample that can be attributed to the presence of Si−O−V bonds. Readsorption of moisture by the calcined sample causes cleavage of Si−O−V bonds followed by structural relaxation and phase separation giving a ^{29}Si spectrum similar to that of the unheated sample with the Q^4 sites resonating close to their uncalcined value.

Reduced Q^4 and increasing numbers of Si−O−V linkages with increasing V concentration results in pore walls that are weak and reactive. Indeed, it seems that if Q^3/Q^4 in uncalcined samples increases beyond 1 stability is severely compromized. Chen et al.[25] have observed that a Q^3/Q^4 ratio less than 1.21 is necessary in MCM-41 for thermal stability. This critical Q^3/Q^4 ratio is reached in the present study for V concentrations less that 13 at. %. In fact, it is only the VS-8 and VS-11 samples that are stable after calcination and rehydration in ambient air.

Following the adsorption of atmospheric moisture by calcined samples, FTIR shows that the V−O−Si/Si−O−Si ratio is reduced to half its precalcination value. This shows that Si−O−V bonds are being cleaved by reaction with water but that some of these linkages remain at least after equilibration in ambient air. Concomitant with the reduction in the number of Si−O−V linkages is the aggregation of initially isolated vanadate polyhedra into polymers and vanadium pentoxide-like clusters.

The fact that reaction of V with atmospheric water results in decomposition of samples containing high V concentrations constitutes further evidence for the homogeneous incorporation of some V since if V were simply grafted to pore walls such a dramatic decomposition on reaction with water would not be expected.

The size, shape, and aggregation of micelles depends on the presence of cosolvents and added electrolytes. It is well-known that for ionic surfactants addition of lower alcohols can lead to a breakdown of micellar aggregates through their effect on solvents while higher alcohols

(27) Gontier, S.; Tuel, A. *Zeolites* **1995**, *15*, 601.
(28) Thomas, J. M.; Klinowski, J. *Adv. Catal.* **1985**, *33*, 199.
(29) Janes, N.; Oldfield, E. *J. Am. Chem. Soc.* **1985**, *107*, 6769.
(30) Walther, K. L.; Wokaun, A.; Handy, B. E.; Baiker, A. *J. Non-Crystalline Solids* **1991**, *134*, 47.
(31) Schraml-Marth, M.; Walther, K. L.; Wokaun, A.; Handy, B. E.; Baiker, A. *J. Non-Crystalline Solids* **1992**, *143*, 93−111.

can bring about modifications in shape and aggregation. Fontell et al.[32] have reported the phase diagram for the ternary system CTA-bromide/water/ethanol, which shows that in this system the liquid crystalline E phase exists up to a maximum ethanol content of 20% beyond which the lamellar phase predominates. In the present study, the abundance of ethanol would suggest that the hexagonal liquid crystalline phase would be significantly destabilized. It is not known how the introduction of silicate anions affect the phase equilibrium. As far as the products are concerned, there is evidence of templating action in this system as shown from XRD and adsorption isotherms, which suggest a disordered pore structure. This further suggests that micelles of some sort are able to form on addition of TEOS or that they form cooperatively after its addition.

This raises the question of what type of pore structure would form from a ternary system involving a higher alcohol such as butanol or pentanol which should promote micellar growth. We are presently investigating this possibility and ways of stabilizing structures formed in alcoholic media.

Although the materials synthesized in the present study are extremely reactive toward water, which causes cleavage of V−O−Si bonds and consequent structural collapse, it is possible that any treatment that improves condensation of SiO_4 and VO_4 tetrahedra could lead to significantly more stable materials.

Conclusion

The synthesis of mesoporous V-silicates with smaller and more disordered pores than MCM-41 has been achieved in ethanolic solution using CTA-vanadate and TEOS precursors and employing base hydrolysis. Condensation of vanadate appears to occur mainly at the micelle interface and at a greater rate than condensation with silicate, resulting in materials in which the pore surfaces are enriched with highly dispersed polymeric vanadium oxo species when the surfactant is removed. Stable materials are formed when the pore walls reach some critical thickness which seems to occur for R less than about 13. Thus, materials with higher surface areas for a given vanadium content and better dispersion of vanadium than can be obtained with solution−sol−gel syntheses in the absence of surfactant. This study has also shown that it may be possible to effect additional control over pore size and possibly also shape by using nonaqueous solvents.

The materials produced in this study compare favorably in terms of vanadium loading, dispersion, and porosity with recently synthesized materials. For instance, MCM-48 in which vanadium was dispersed on the surfaces using a vanadium alkoxide solution[23] and mesoporous sol−gel derived silicates in which vanadium is incorporated also using a vanadium alkoxide followed be supercritical drying.[11] Since vanadium alkoxides are costly and supercritical drying is a low-volume process the advantage of the present materials may be that comparably high vanadium loadings and dispersions can be achieved using cheap vanadium salts and surfactants without the need for special drying conditions.

Acknowledgment. We wish to thank Denis Bogsányi for assistance with recording the FTIR and diffuse reflectance spectra. We are also grateful to Dr. Richard Bramley for access to the pulsed EPR spectrometer.

CM960621K

(32) Fontell, K.; Khan, A.; Lindstrom, B.; Maciejewska, D.; Puang-Ngern, S. *Colloid Polym. Sci.* **1991**, *269*, 727.